ELSEVIER

Journal of Luminescence 99 (2002) 325–334

JOURNAL OF LUMINESCENCE

www.elsevier.com/locate/jlumin

Luminescence of nanocrystalline ZnS:Cu^{2+}

Ageeth A. Bol*, Joke Ferwerda, Jaap A. Bergwerff, Andries Meijerink

Chemistry and Physics of Condensed Matter, Debye Institute, Utrecht University, P.O. Box 80 000, 3508 TA Utrecht, The Netherlands

Received in revised form 9 May 2002; accepted 9 May 2002

Abstract

Temperature dependent luminescence and luminescence lifetime measurements are reported for nanocrystalline ZnS:Cu^{2+} particles. Based on the variation of the emission wavelength as a function of particle size (between 3.1 and 7.4 nm) and the low quenching temperature ($T_q = 135$ K), the green emission band is assigned to recombination of an electron in a shallow trap and Cu^{2+}. The reduction in lifetime of the green emission (from 20 μs at 4 K to 0.5 μs at 300 K) follows the temperature quenching of the emission. In addition to the green luminescence, a red emission band, previously only reported for bulk ZnS:Cu^{2+}, is observed. The red emission is assigned to recombination of a deeply trapped electron and Cu^{2+}. The lifetime of the red emission is longer (about 40 μs at 4 K) and the quenching temperature is higher.

PACS: 78.55.et; 78.66.hf

Keywords: ZnS:Cu; Nanocrystals; Time resolved spectroscopy

1. Introduction

The first observation of the luminescence of ZnS:Cu was in 1866, when a young French chemist, Théodore Sidot, observed that ZnS crystals grown by a sublimation method exhibited phosphorescence [1]. From the present knowledge, one can conclude that these crystals, which were later called Sidot's blende, contained a small quantity of copper that was responsible for the observed phosphorescence.

After the research of Sidot it became gradually clear that when ZnS powders are fired in the presence of a small amount of metallic salt the ZnS emits light characteristic for the incorporated impurity. In the 1920s it was established that a small amount of copper incorporated in ZnS produces a green luminescence. During the period from the 1950s to the 1970s the research on the luminescence of bulk ZnS:Cu expanded. This material turned out to be a good cathode ray tube (CRT) phosphor and was applied in for example oscilloscopes. Besides that, the electroluminescence (EL) of bulk ZnS:Cu has been widely studied for possible applications in EL devices.

For bulk ZnS:Cu five emissions are observed: a UV, blue, green, red and IR emission. It is generally

*Corresponding author. Current address: Philips Research, Prof. Holstlaan 4 (WA11), 5656 AA Eindhoven, Netherlands. Tel.: +31-40-2742271; fax: +31-40-2744282.

E-mail address: ageeth.bol@philips.com (A.A. Bol).

0022-2313/02/$ - see front matter
PII: S0022-2313(02)00350-2

believed that copper incorporates in ZnS on a Zn^{2+} site as Cu^{2+} ($3d^9$). In the tetrahedral crystal field of the four S^{2-} ligands the $3d^9$ ground-state splits into higher lying t_2 levels and lower lying e levels (see Fig. 1) [2]. The observed IR emission ($\sim$1450 nm) corresponds to the transition from the t_2 level to the e level [2]. When an electron is excited to the conduction band, and subsequently trapped by shallow (delocalised) donor levels, a green luminescence can occur, by recombination at the Cu impurity (see Fig. 1) [2]. This so-called G-Cu emission has been studied extensively by Shionoya and co-workers (e.g., [3]). The red emission (R-Cu) is assigned to the recombination of an electron from a deep (localised) donor level (e.g., S^{2-} vacancy) at the copper site [4].

One should be careful in considering energy level diagrams as shown in Fig. 1. The picture suggests that one could expect two emission bands for recombination from the shallowly or deeply trapped electron: one for a transition to the e levels of Cu^{2+} and one for a transition to the t_2 levels of Cu^{2+}. In several publications this is in fact suggested [2]. However, the problem of energy level diagrams like Fig. 1 is that the valence state of Cu^{2+} before recombination is included. After recombination Cu^{+} ($3d^{10}$) is formed which has a non-degenerate $^1S_0$ ($^1A_1$) ground state. The green luminescence arises from the transition from a high-energy state (trapped electron and Cu^{2+}) to a lower-energy state (Cu^{+}). The final state is non-degenerate and thus a single emission band is expected.

The origin of the blue copper emission (B-Cu) is not clear. Possibly a centre formed by the spatial association of a substitutional Cu and an interstitial Cu is involved [3]. The defect related ZnS emission (also known as the self-activated (SA) emission), which is also observed for undoped ZnS, is positioned in the UV/blue.

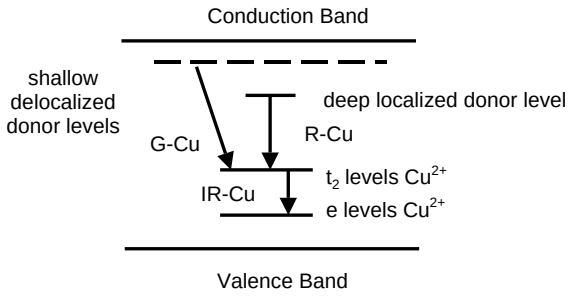

Fig. 1. Schematic energy level diagram of $ZnS:Cu^{2+}$ (see Ref. [2] for a more detailed overview).

Lately, the optical properties of doped semiconductor nanoparticles have gained much attention [5–7]. Semiconductor nanoparticles with dimensions smaller than the bulk exciton show unique optical properties, which depend strongly on the size [8–11]. The change of the electronic structure can be explained by strong confinement of the charge carriers in all three dimensions. Besides the size quantisation, surface effects are also known to influence the optical properties of these nanoparticles.

Recently, the luminescence of nanocrystalline ZnS:Cu has been investigated [12–16]. Due to the large surface to volume ratio of the nanoparticles, charge carriers can be injected efficiently into these materials. This could make nanocrystalline semiconductors better suited for EL devices than bulk materials. Prior to application of these materials it is important to investigate the effects of the particle size on the luminescence of these materials.

For nanocrystalline ZnS:Cu only a green luminescence is reported [12–16], while for bulk ZnS:Cu also UV/blue, red and IR emissions are observed. The spectral position reported for the green emission in the papers on nanocrystalline ZnS:Cu varies from 425 nm [12] to 525 nm [14]. The measurements are limited to room temperature and the lifetime of the observed luminescence has not been investigated. This article reports on the temperature dependence (4 K−RT) of the luminescence of nanocrystalline ZnS:Cu and the lifetime of the luminescence was investigated as well. In addition, the influence of the particle size (band gap), and the synthesis conditions on the luminescence are studied. For the first time a red emission is reported for nanocrystalline ZnS:Cu.

2. Experimental

The synthesis route followed to make nanocrystalline $ZnS:Cu^{2+}$ resembles methods, which are nowadays commonly used for the synthesis of

nanocrystalline II–VI semiconductors. The method used for the synthesis of nanocrystalline ZnS:Cu^{2+} coated with sodiumpolyphosphate (PP) is very similar to the one we used for the synthesis of nanocrystalline ZnS:Mn^{2+} and ZnS:Pb^{2+} [7,17]. 10 ml 1 M $Zn(CH_3COO)_2.2H_2O$ and 1 ml 0.01 M $Cu(CH_3COO)_2.H_2O$ were added to an aqueous solution of 10.2 g $Na(PO_3)_n$ (Aldrich, 96%, $n \sim 10$). The total volume after the addition was 90 ml. After about 10 min of stirring, 10 ml of a 1 M $Na_2S.9H_2O$ solution was injected into the solution. Immediately after the injection of the Na_2S solution a turbid white fluid was obtained. Then the particles were centrifuged, rinsed with distilled water and ethanol, and dried in vacuum (sample A). To increase the particle size a small amount of sample A was heated in a nitrogen atmosphere for 10 min at 450°C (sample B). To investigate the influence of the sulphide concentration used in the synthesis on the luminescence of nanocrystalline ZnS:Cu^{2+}, sample C was prepared using 8 ml of 1 M $Na_2S.9H_2O$ (S^{2-} deficiency) and sample D using 13.3 ml of 1 M $Na_2S.9H_2O$ (S^{2-} excess).

X-ray powder diffraction patterns of the nanoparticles were obtained with a Philips PW 1729 X-ray generator with Cu Kα radiation ($\lambda = 1.542$ Å). From the line width the particle diameter was calculated using the Scherrer formula [18]. A Perkin-Elmer Optima-3000 was used to determine the chemical composition of the samples by inductively coupled plasma analysis (ICP). Diffuse reflection spectra were measured using a double beam Perkin-Elmer Lambda 16 UV/VIS spectrophotometer.

Emission and excitation spectra were recorded on a SPEX Fluorolog spectrofluorometer model F2002, equipped with two double grating 0.22 m monochromators (SPEX 1680) and a 450 W Xenon lamp as a excitation source. The emission was detected with a cooled Hamamatsu R928 photomultiplier. In some cases an ARC Spectro Pro®-300i monochromator and a Princeton Instruments CCD camera were used to record emission spectra. The experimental error in both excitation and emission spectra is smaller than 1 nm (smaller than 0.01 eV in the measured spectral region).

For lifetime measurements at an excitation wavelength of 355 nm the third harmonic of a Quanta Ray Nd:YAG laser was used. The emission was detected by an ARC Spectro Pro®-300i monochromator and a RCA c31034 photomultiplier tube. Decay curves were measured with a Tektronix 2440 digital oscilloscope. Temperature dependent measurements were performed using an Oxford Instruments liquid helium flow cryostat for temperatures ranging from 4.2 K to room temperature.

3. Results and discussion

3.1. Characterisation

For the interpretation of the luminescence spectra it is important to characterise the ZnS:Cu^{2+} samples. Here, UV–VIS reflection spectroscopy, X-ray diffraction and inductively ICP have been used to study the absorption characteristics, size, Zn/S ratio and incorporation of Cu in the ZnS:Cu particles obtained for different synthesis conditions. In Table 1 the average particle diameter of samples A–D and the results of the ICP analysis are shown.

Fig. 2 shows the reflection spectra of samples A, C and D. These three samples show an absorption band around 300 nm with a shoulder around 360 nm. In addition, a broad weak absorption extending from 450 to 700 nm is visible. This broad absorption band and the shoulder around 360 nm are absent in undoped nanocrystalline ZnS and increase with increasing S^{2-} (see Fig. 2) and Cu^{2+}

Table 1
Average particle diameter, molar Zn/S ratio in reaction vessel and the Zn/S ratio and Cu concentration in the sample determined by ICP analysis of samples A–D

Sample	Diameter (nm)	Molar Zn/S ratio reaction vessel	Molar Zn/S ratio ICP	Cu concentration (at%)
A	4.1	1	1.15	0.123
B	7.4	1	1.13	0.121
C	3.1	1.25	1.36	0.115
D	4.5	0.75	1.03	0.098

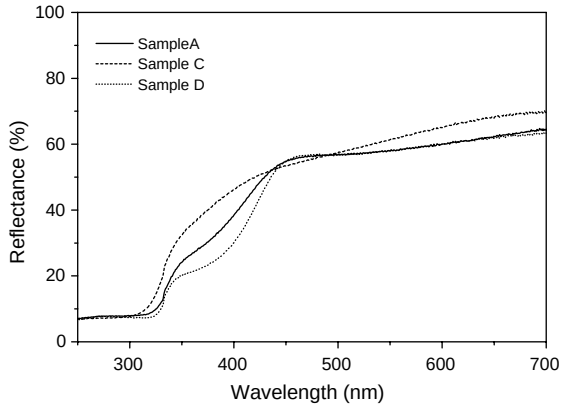

Fig. 2. UV–VIS reflection spectra of nanocrystalline ZnS:Cu (samples A, C and D).

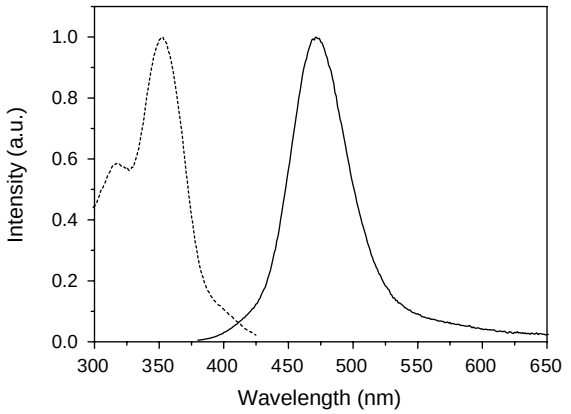

Fig. 3. Emission (solid line) and excitation spectrum (dashed line) of nanocrystalline ZnS:Cu^{2+} (sample A) measured at 4 K. The solid line represents the emission spectrum measured at an excitation wavelength of 350 nm. The dashed line represents the excitation spectrum measured for 470 nm emission.

concentration in the reaction vessel. The absorption around 360 nm is also visible in the excitation spectrum of the green and red emission from nanocrystalline ZnS:Cu (see Fig. 3) and is assigned to a transition involving the Cu^{2+} ion in the ZnS nanocrystal. The weak absorption band extending from 400 to 750 nm is possibly caused by the formation of small amounts of CuS/Cu_2S (black). The broad band around 300 nm is assigned to host lattice absorption. Due to quantum size effects this band has shifted to higher energies compared to the absorption band of bulk ZnS.

The average particle diameter was calculated from the XRD pattern of the sample using Scherrer's formula [18]. Earlier [17] we have found that the average particle diameter obtained from XRD patterns is in good agreement with the average particle diameter obtained from high-resolution TEM pictures. The size distribution obtained with the described preparation method is normally quite large (FWHM about 50% [17]). When sample A is subjected to a heat treatment (10 min at 450°C in a nitrogen atmosphere) the average particle size increases from 4.1 nm (sample A) to 7.4 nm (sample B). Due to the heat treatment the colour of the sample changed from almost white to brown, possibly due to the formation of a coppersulphide phase at elevated temperature.

As can be deduced from Table 1 the sulphide concentration used in the synthesis influences the average particle size of the ZnS nanoparticles. The sample made with a deficiency of S^{2-} (sample C) has the smallest average particle diameter (3.1 nm), while the sample made with an excess of S^{2-} (sample D) has an average particle diameter of 4.5 nm. A relation between the particle size and the Zn/S precursor ratio has been reported before by Suyver et al. [19]. This increase in the average particle diameter with increasing sulphide concentration is also observable in the UV–VIS reflectance spectra (see Fig. 2). When the sulphide concentration increases (yielding a larger average particle size) the host lattice absorption band around 300 nm shifts to lower energies due to quantum size effects.

The results of the ICP analysis (see Table 1) show that the amount of copper incorporated in the ZnS nanoparticles is similar for all four samples. In all cases the amount of copper in the reaction vessel was 0.1 at% relative to the zinc concentrations. From the ICP analysis it can be concluded that the relative amount of copper incorporated in the nanoparticles is the same (around 0.1 at% relative to zinc) as was present in the reaction vessel. Furthermore, from Table 1 it can be deduced that by increasing the molar Zn/S ratio present in the reaction vessel, the molar Zn/S ratio inside the nanoparticles increases as well. However, in all cases the Zn/S ratio inside

the nanoparticles is higher than was initially present in the reaction vessel.

3.2. Luminescence spectroscopy

In Fig. 3 the excitation and emission spectra of sample A measured at 4 K are depicted. Upon 350 nm excitation a green emission peaking at 470 nm is observed. The excitation spectrum of the green emission band reveals that this emission can be most efficiently excited at an excitation wavelength of 350 nm. From Fig. 3 it is clear that the green emission can also be excited at an excitation wavelength of 320 nm (host lattice absorption). This green emission probably originates from the recombination of an electron from a shallow delocalised donor level just below the conduction band at the Cu^{2+} impurity [2], similar to the mechanism proposed for the green Cu emission in bulk ZnS:Cu^{2+}. Excitation of the green luminescence can occur by excitation over the band gap ($\lambda_{exc} = 320$ nm). Alternatively, local excitation of an electron of Cu^{2+} to the conduction band can also give rise to green emission, as is evident from the strong excitation band at 355 nm (see Fig. 3). The assignment of this excitation band to a local excitation involving Cu^{2+} is confirmed by the diffuse reflection spectra (Fig. 2) where (only) for the Cu doped ZnS samples an absorption band around 360 nm is observed.

At room temperature a red emission around 600 nm is also visible upon sub-band excitation ($\lambda_{exc} = 345$ nm) (see Fig. 4). This red emission is also reported for bulk ZnS:Cu^{2+} [4]. For nanocrystalline ZnS:Cu^{2+} this emission has never been observed before. Based on previous publications on bulk ZnS:Cu^{2+} [2,4] the red emission is assigned to a transition between a deep localised donor level (possibly related to a S^{2-} vacancy) and the Cu^{2+} impurity, yielding Cu^{+}, in analogy with the situation in bulk ZnS:Cu^{2+} [2].

In Fig. 5 the temperature dependence of the emission spectrum ($\lambda_{exc} = 350$ nm) of sample A is shown. For samples C and D similar results were obtained. As can be seen in this figure the green emission quenches with increasing temperature. At room temperature the green emission has almost quenched completely and the weak red emission

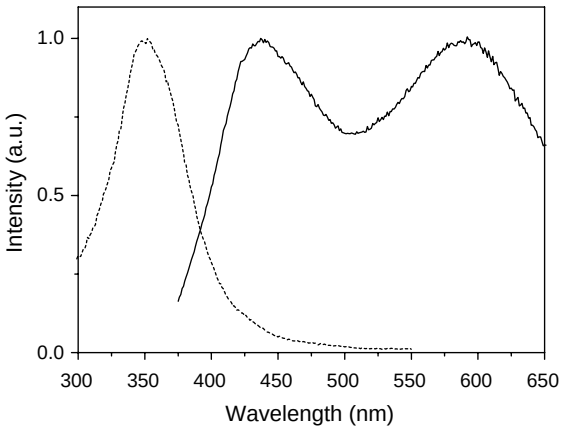

Fig. 4. Emission (solid line) and excitation spectrum (dashed line) of nanocrystalline ZnS:Cu (sample A) measured at room temperature. The solid line represents the emission spectrum measured at an excitation wavelength of 345 nm. The dashed line represents the excitation spectrum measured for 600 nm emission.

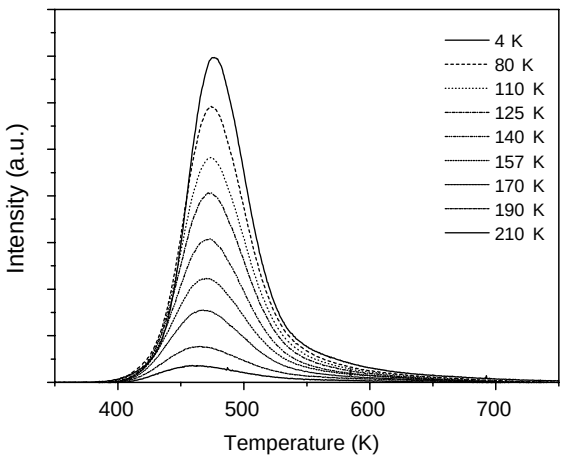

Fig. 5. Temperature dependence of the emission ($\lambda_{exc} = 350$ nm) of nanocrystalline ZnS:Cu (Sample A).

becomes visible (see Fig. 4). From Fig. 5 it is clear that the green emission shifts to higher energies with increasing temperature (shift ~ 0.1 eV between 4 and 300 K). This is in contrast with the green emission of bulk ZnS:Cu. In bulk ZnS:Cu the green emission shifts to lower energies with increasing temperature [3] (shift ~ 14 meV). Shionoya and co-workers correlated this shift with the shift of the conduction band to lower energies with increasing temperature. The shallow traps from

which the green emission originates shift together with the conduction band to lower energy, which causes the small red shift of the emission spectrum for bulk ZnS:Cu. It is not clear why the G-Cu emission in the ZnS:Cu nanocrystals shifts to the blue. The temperature dependence of the band gap is similar for bulk and nanocrystalline semiconductors [19], so a similar red shift would be expected.

The temperature dependence of the emission spectra of sample B (heat-treated sample) measured at 352 nm excitation is depicted in Fig. 6. As is clear from Fig. 6 the green emission quenches at lower temperatures than the red emission. This is consistent with the model proposed for bulk ZnS:Cu [2] in which the green emission originates from shallow delocalised traps and the red emission from deep localised traps. Since the shallow delocalised traps are situated just below the conduction band, these traps are thermally emptied at relative low energies. More energy is needed to empty the deep traps responsible for the red emission.

As a consequence the red emission quenches at much higher temperatures. As far as can be deduced, the red emission does not shift with increasing temperature. For the red emission of bulk ZnS:Cu a blue shift (shift ~ 36 meV) was reported with increasing temperature [3]. This shift was explained with the configurational co-ordinate model for a localised luminescence centre. With increasing temperature higher vibrational levels of the excited state will be occupied, which results in a shift of the emission spectrum to higher energies [3].

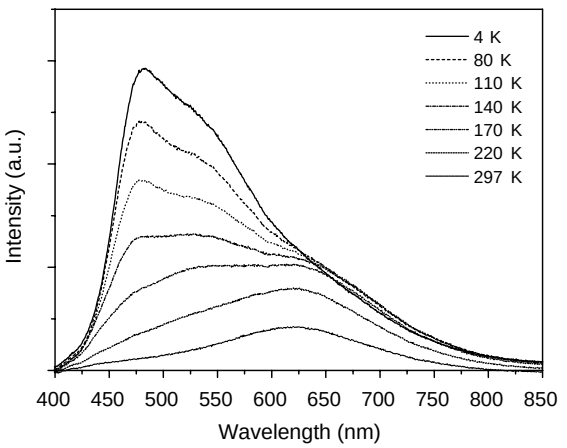

Fig. 6. Temperature dependence of the emission ($\lambda_{exc} =$ 352 nm) of heat-treated nanocrystalline ZnS:Cu (Sample B).

The quenching temperature T_q is defined as the temperature at which the intensity of the emission has decreased to half of its maximum intensity. The quenching temperature of the green emission is ≈ 135 K for all samples. This temperature is not dependent on the size of the nanoparticles. The position of delocalised shallow traps shift together with the conduction band to lower energies with increasing particle size. The energy difference between the shallow traps and the conduction band will therefore not change by varying the particle size, and the quenching temperature of the green emission is the same for all samples.

Since the red emission originates from deep localised traps it is possible that the quenching of the red emission is dependent on the particle size. However, since the green emission is very intense at low temperatures, the red emission is hardly observable up till 200 K for most samples (except sample B, see Figs. 5 and 6). It is, therefore, not possible to determine the quenching temperature for the red emission as a function of particle size.

By comparing Fig. 5 with Fig. 6 it can be noticed that due to a heat treatment of sample A the intensity of the red emission drastically increases. Shionoya and co-workers [4] proposed that the red emission involved an S^{2-} vacancy deep in the band gap and the Cu impurity. The heat treatment may result in an increase of the S^{2-} vacancy concentration or lead to an increase of association of S^{2-} vacancies and Cu^{2+} ions, resulting in an increase of the red emission intensity.

In Fig. 7 the emission and excitation spectra of samples A–D measured at 4 K are plotted on an energy scale. In Table 2 the average particle sizes of the samples are shown together with the maxima of the excitation and emission spectra.

As is clear from Table 2 and Fig. 7 the spectral positions of both the emission and the excitation spectrum of the green emission is dependent on the particle size. With increasing particle size the spectral position of both the emission and

excitation spectra shift to lower energy. Due to quantum size effects the conduction band shifts to lower energy with increasing particle size. The shallow delocalised traps, from which the green emission originates, shift together with the conduction band to lower energies. Therefore, a red shift of both the emission and excitation spectrum with increasing particle size is observed.

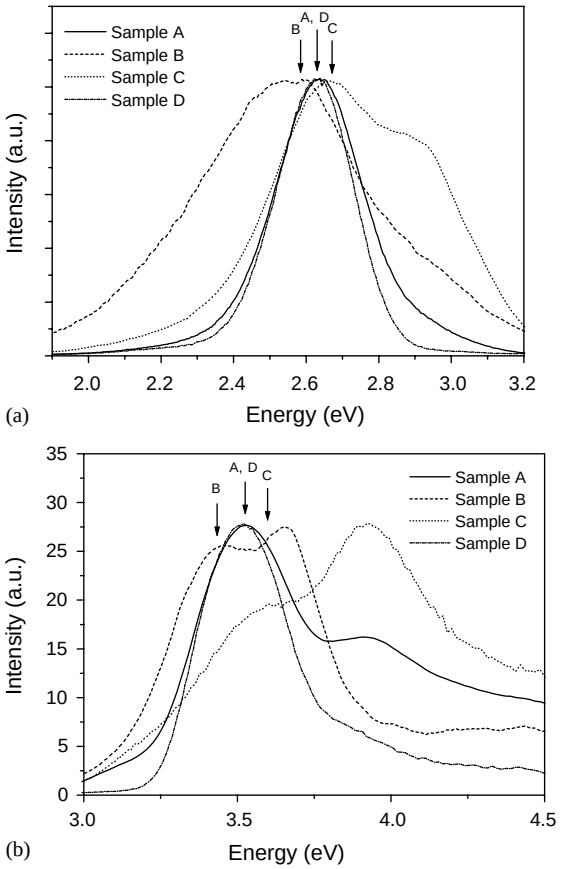

Fig. 7. Excitation and emission spectra measured at 4 K for nanocrystalline ZnS:Cu plotted on an energy scale. The solid, dashed, dotted and dash-dotted line depict the emission and excitation spectra of samples A, B, C and D, respectively. (a) Emission spectra (normalised at maximum intensity) measured for $\lambda_{exc} = 350$ nm. (b) Excitation spectra (normalised at maximum intensity) measured for $\lambda_{em} = 470$ nm.

Using Eq. (1) the size of the band gap (E) of samples A–D has been calculated:

$$E = E_g + \frac{\pi^2\hbar^2}{2m_0R^2}\left(\frac{1}{m_e^*} + \frac{1}{m_h^*}\right) - \frac{1.8e^2}{4\pi\varepsilon_0\varepsilon_\infty R} \quad (1)$$

where R is the radius of the semiconductor particle, E_g the band gap of the bulk semiconductor (3.7 eV for ZnS [21]), and m_e^* and m_h^* are the effective masses of the electron and the hole, respectively. The results of the calculations are shown in Table 2. Due to quantum size effects the band gap energy increases with decreasing particle size. As can be concluded from Table 2 the shifts in the calculated band gap energy with decreasing particle size are larger than the observed shifts of the emission and excitation spectra. The shift of the band gap energy is caused by the shift of the conduction band to higher energy and the shift of the valence band to lower energy. Assuming that the effective mass of the electron in ZnS is $0.25m_e$ [22] and the effective mass of the hole in ZnS is $0.59m_e$ [22] the energy shift of the conduction band is larger than the energy shift of the valence band. With respect to this the observed shift in the emission and excitation spectra with decreasing particle size, is smaller than expected from formula (1). One reason could be that this formula is derived for the strong confinement regime [11]. Samples A–D are in the weak confinement regime. Another possible explanation could be that the energy of the shallow trap states is less influenced

Table 2
Average particle size, band gap energy and the spectral position of the excitation and emission maximum of samples A–D

Sample	Average particle size[a] (nm)	Calculated band gap energy[b] (eV)	Spectral position excitation maximum (eV)	Spectral position emission maximum (eV)
C	3.1	4.64	3.58	2.67
A	4.1	4.24	3.53	2.64
D	4.5	4.12	3.53	2.63
B	7.4	3.84	3.45	2.60

[a] Determined from XRD.
[b] Calculated with Eq. (1).

by quantum confinement than the conduction band.

The currently observed shift of the emission band with decreasing particle size can possibly explain some of the reported differences in the spectral position of the green emission. However, other factors, like other traps (Al^{3+}, Cl^{-}), synthesis conditions or overlap with the blue ZnS related emission band probably also contribute to these differences.

From Fig. 7(a) it can also be deduced that the relative intensities of the green and semiconductor related emission change upon changing the sulphide concentration and after the heat treatment. The ZnS related emission (around 420 nm, 2.9 eV) of sample C is relatively intense compared with the G-Cu emission. Since the amount of Cu incorporated in the nanocrystals is about the same for all samples, this observation is not due to a smaller amount of Cu incorporated in the nanoparticles. The ZnS related SA emission has been proposed to be related to S^{2-} vacancies. In the case of a Zn/S ratio larger than 1 the S^{2-} vacancy concentration will be higher and a stronger defect emission in the UV/blue is expected. Also for sample B, where a higher S^{2-} vacancy concentration can be expected, the SA emission band around 2.9 eV is visible. Similar results have been reported by Suyver et al. [20].

3.3. Lifetime measurements

To investigate the origin of the green and red emission in more detail lifetime measurements were performed. A typical decay curve measured for the green emission of sample A is shown in Fig. 8. The tails of the decay curves were fitted to a single exponential decay function. In Fig. 9 the lifetime of the green emission of sample A is plotted as a function of temperature. The intensity of the green emission of sample A as a function of temperature is shown as well. For the other samples similar results were obtained. Going from 4 K to room temperature the lifetime of the green emission decreases form 20 to 0.5 μs. The temperature dependence of the lifetime of the green emission is the same as the temperature dependence of the intensity of the green emission. This

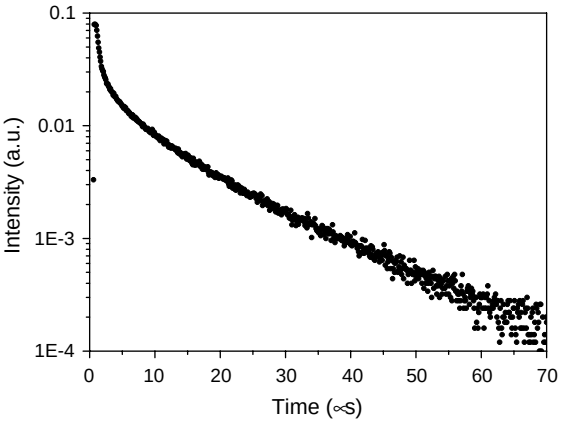

Fig. 8. Typical decay curve measured for the green emission ($\lambda_{em} = 470$ nm) of sample A at 160 K under 355 nm excitation.

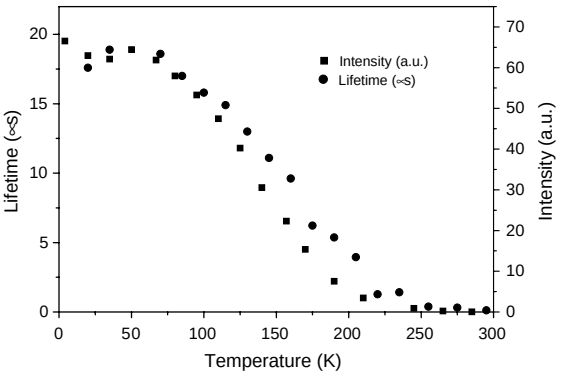

Fig. 9. Intensity and lifetime of the green emission ($\lambda_{em} = 470$ nm) of sample A as a function of temperature measured under 355 nm excitation.

behaviour is typical for the situation where the lifetime is shortened by a faster non-radiative decay from the excited state at higher temperatures.

In the present situation the emission intensity and the emission lifetime are reduced by the thermal excitation of electrons from the shallow traps to the conduction band. The quenching temperature of the lifetime is not influenced by the particle size, since for all samples the quenching temperature is the same. This is in line with the idea that the shallow traps shift to higher energy together with the conduction band as the particle size decreases. Charge carriers trapped in shallow traps are still delocalised. The spatial extension of

the trapped charge carriers depends on the trap depth. Deeper trapping corresponds to stronger localisation of the trapped charge carriers. Due to the delocalised nature of the shallowly trapped charge carriers also the energy of the traps shifts as the charge carriers experience confinement due to the size of the nanocrystals. This shift will be smaller as the trap depth increases. For deeply trapped charge carriers the energy depends only on the local surroundings and no shift as a function of particle size is expected.

Since the red emission of samples A, C and D is very weak relative to the intensity of the green emission at low temperatures it was not possible to measure the lifetimes of the red emission as a function of temperature for these samples. For sample B the red emission is relatively strong (see Fig. 6).

In Fig. 10 a typical decay curve measured for the red emission of sample B is shown. The decay curves measured at 600 nm have a fast component that most probably originates from the tail of the green emission and a slower component, which is due to the decay of the red emission.

Fig. 11 shows the lifetimes of the red emission (slow component) as a function of temperature. At low temperatures, the lifetime of the red emission is about 40 μs, close to the value reported for the red emission in bulk ZnS:Cu^{2+} ($\sim$50 μs [23]). As is clear form Fig. 11 both the lifetime and the intensity of the red emission decrease at rather high temperatures (>200 K). This is consistent with the model in which it is assumed that the red emission originates from deep localised traps.

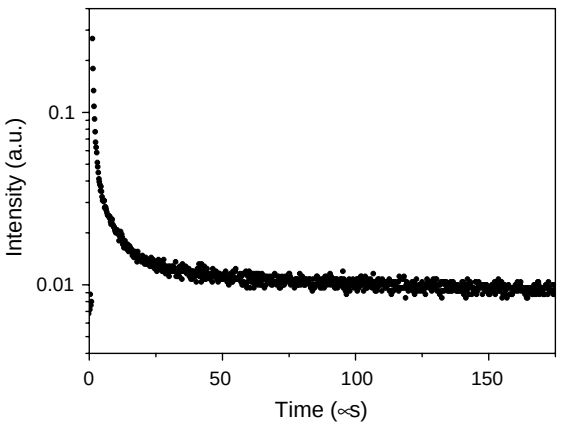

Fig. 10. Typical decay curve measured for the red emission ($\lambda_{em} = 600$ nm) of sample B at 4 K under 355 nm excitation.

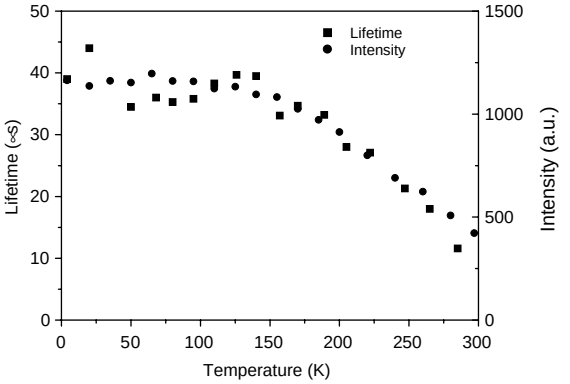

Fig. 11. Intensity and lifetime of the red emission ($\lambda_{em} = 600$ nm) of sample B as a function of temperature measured under 355 nm excitation.

4. Conclusions

Luminescence measurements on nanocrystalline ZnS:Cu^{2+} particles as a function of particle size and temperature indicate that the green emission from these particles is due to recombination of a shallowly trapped electron and Cu^{2+}. The emission shifts to slightly higher energies in the smaller particles due to quantum size effects experienced by the delocalised shallowly trapped electrons. The quenching temperature for the emission is about 135 K. Temperature quenching is accompanied by a decrease in the emission lifetime from 20 μs at 4 K to 0.5 μs at 300 K. In addition, a red emission band is observed which is assigned to recombination of a deeply trapped electron and Cu^{2+}. The red emission is characterised by a longer lifetime (40 μs at 4 K) and a higher quenching temperature. The intensity of the red emission band is strongly dependent on the synthesis procedure.

References

[1] E. Becquerel, C. R. Acad. Sci. 62 (1866) 999.
[2] P. Peka, H.J. Schulz, Physica B 193 (1994) 57.

[3] S. Shionoya, T. Koda, K. Era, H. Fujiwara, J. Phys. Soc. Japan 19 (1964) 1157.
[4] S. Shionoya, K. Urabe, T. Koda, K. Era, H. Fujiwara, J. Phys. Chem. Solids 27 (1966) 865.
[5] R.N. Bhargava, D. Gallagher, Phys. Rev. Lett. 72 (1994) 416.
[6] G. Counio, T. Gacoin, J.P. Boilot, J. Phys. Chem. B 102 (1998) 5257.
[7] A.A. Bol, A. Meijerink, Phys. Rev. B 58 (1998) R15997.
[8] R. Rossetti, R. Hull, J.M. Gibson, L.E. Brus, J. Chem. Phys. 82 (1985) 552.
[9] L. Brus, J. Phys. Chem. 90 (1986) 2555.
[10] A. Henglein, Chem. Rev. 89 (1989) 1861.
[11] Y. Wang, N. Herron, J. Phys. Chem. 95 (1991) 525.
[12] A.A. Koshravi, M. Kundu, L. Jatwa, S.K. Deshpande, U.A. Bhagwat, M. Sastry, S.K. Kulkarni, Appl. Phys. Lett. 67 (1995) 2702.
[13] J. Huang, Y. Yang, S. Xue, B. Yang, S. Liu, J. Shen, Appl. Phys. Lett. 70 (1997) 2335.
[14] W. Que, Y. Zhou, Y.L. Lam, Y.C. Chan, C.H. Kam, B. Liu, L.M. Gan, C.H. Chew, G.Q. Xu, S.J. Chua, S.J. Xu, F.V.C. Mendis, Appl. Phys. Lett. 73 (1998) 2727.
[15] L. Sun, C. Liu, C. Liao, C. Yan, Solid State Commun. 111 (1999) 483.
[16] M. Wang, L. Sun, X. Fu, C. Liao, C. Yan, Solid State Commun. 115 (2000) 493.
[17] A.A. Bol, A. Meijerink, Phys. Chem. Chem. Phys. 3 (2001) 2105.
[18] B.D. Cullity, Elements of X-ray Diffraction, Addison-Wesley, Reading, MA, 1978, p. 102.
[19] J.F. Suyver, S.F. Wuister, J.J. Kelly, A. Meijerink, Phys. Chem. Chem. Phys. 2 (2000) 5445.
[20] J.F. Suyver, S.F. Wuister, J.J. Kelly, A. Meijerink, Nano Lett. 1 (2001) 429.
[21] W.M. Yen, S. Shionoya (Eds.), Phosphor Handbook, CRC Press, Boca Raton, FL, 1999.
[22] K. Sooklal, B.S. Cullum, S.M. Angel, C.J. Murphy, J. Phys. Chem. 100 (1996) 4551.
[23] K. Osada, H. Iguchi, I. Iwasaki, M. Yano, M. Mikami, N. Okamoto, J. Gotohda, Kinki Daigaku Rikogakubu Kenkyu Hokoku 26 (1990) 63.